Molecular Crystals and Liquid Crystals
Publication details, including instructions for authors and subscription information:
http://www.tandfonline.com/loi/gmcl20

Synthesis and Physical Properties of Ferrocene Derivatives (XXIII) Phase Transition and Unique Molecular Structure of Monosubstituted Ferrocene Derivatives

Naotake Nakamura [a], Kazuya Hiro* [a], Masako Nishikawa** [a], Takashi Okabe*** [a] & Kenjiro Uno [a]

[a] Department of Applied Chemistry, College of Science and Engineering, Ritsumeikan University, Kusatsu, Shiga, Japan

To cite this article: Naotake Nakamura, Kazuya Hiro*, Masako Nishikawa**, Takashi Okabe*** & Kenjiro Uno (2010): Synthesis and Physical Properties of Ferrocene Derivatives (XXIII) Phase Transition and Unique Molecular Structure of Monosubstituted Ferrocene Derivatives, Molecular Crystals and Liquid Crystals, 516:1, 122-131

To link to this article: http://dx.doi.org/10.1080/15421400903400829

Mol. Cryst. Liq. Cryst., Vol. 516: pp. 122–131, 2010
Copyright © Taylor & Francis Group, LLC
ISSN: 1542-1406 print/1563-5287 online
DOI: 10.1080/15421400903400829

Taylor & Francis
Taylor & Francis Group

Synthesis and Physical Properties of Ferrocene Derivatives (XXIII): Phase Transition and Unique Molecular Structure of Monosubstituted Ferrocene Derivatives

NAOTAKE NAKAMURA, KAZUYA HIRO*,
MASAKO NISHIKAWA**, TAKASHI OKABE***,
AND KENJIRO UNO

Department of Applied Chemistry, College of Science and Engineering,
Ritsumeikan University, Kusatsu, Shiga, Japan

The monosubstituted ferrocene derivatives, ω-[4-(4-methoxyphenoxycarbonyl) phenoxy]alkoxycarbonyl ferrocene, were synthesized in order to compare the liquid crystallinity to that of disubstituted ferrocene derivatives, 1,1′-bis[ω-[4-(4-methoxyphenoxycarbonyl)phenoxy]alkoxycarbonyl]ferrocene. Some of the monosubstituted ferrocene derivatives containing relatively longer flexible spacer showed the liquid crystalline phase, nematic and/or smectic phases. The crystal structure of 2-[4-(4-methoxyphenoxycarbonyl)phenoxy]ethoxycarbonyl ferrocene was determined by X-ray diffraction method using a single crystal. The molecular structure revealed a bent structure that is almost a half of "Z" shaped molecular structure of 1,1′-bis[2-[4-(4-methoxyphenoxycarbonyl)phenoxy]ethoxycarbonyl]ferrocene.

Keywords Crystal structure; ferrocene; liquid crystal; metallomesogen; monosubstituted ferrocene derivative

Introduction

Ferrocene, one of the metallocenes, contains an iron atom. As it has a thermal stability and an aromaticity, the substitution reaction easily occurs under a mild reaction condition. If a mesogenic group is introduced in the ferrocene molecule,

---

*Present address: TOYOBO Co., Ltd. 2-8, Dojima Hama 2-chome, Kita-ku, Osaka 530-8230, Japan.

**Present address: Molex Japan Co., Ltd. 1-5-4, Fukami-higashi, Yamato, Kanagawa 242–8585, Japan.

***Present address: Unitika LTD, 31-3, Uji-hinojiri, Uji-city, Kyoto 611-0021, Japan.

A High-Tech Research Center Project for Private Universities matching fund subsidy from Ministry of Education, Culture, Sports, Science and Technology, 2006–2010 is gratefully acknowledged for partial financial support of the present work. We are grateful to Assoc. Prof. T. Hanasaki, Ritsumeikan University for his useful discussion on the molecular design, and Mr. T. Takamatsu, Ritsumeikan University for his support of structure analysis.

Address correspondence to Naotake Nakamura, Department of Applied Chemistry, College of Science and Engineering, Ritsumeikan University, 1-1-1, Nojihigashi, Kusatsu, Shiga 525-8577, Japan. E-mail: nakamura@sk.ritsumei.ac.jp

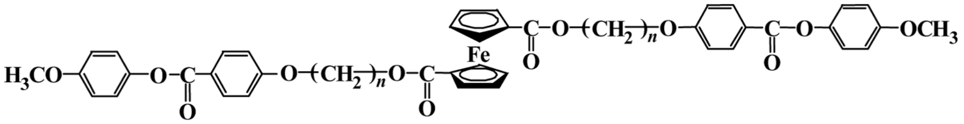

Figure 1. General structure of bMAF-*n*.

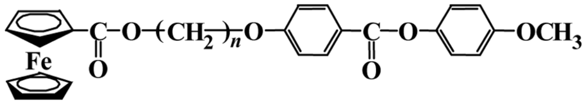

Figure 2. General structure of mMAF-*n*.

the ferrocene derivative may show a liquid crystallinity. The derivative is one of the metallomesogens, which shows unique physical properties [1,2].

In our laboratory, a series of disubstituted ferrocene derivatives, 1,1′-bis[ω-[4-(4-methoxyphenoxycarbonyl)phenoxy]alkoxycarbonyl]ferrocene (abbreviated hereafter as bMAF-*n*, $n = 2\sim12$, where n is the number of carbon atoms in the methylene chain) were prepared [3,4]. A general structure of bMAF-*n* is shown in Figure 1. In the homologues, bMAF-3 and 5∼12 show liquid crystalline phases. In contrast, bMAF-2 and 4 have no liquid crystalline phase [3,4]. We have already determined the crystal structures of bMAF-2 [5], 3 [6], 5 [7], 9 [8] and 10 [9]. The molecular structure of bMAF-2 [5] was "Z" shaped conformation, bMAF-3 [6] was "U" shaped one, and that of bMAF-5 [7] was "S" shaped one, whereas the molecular structures of bMAF-9∼10 were "U" shaped one. The two substituents in the "Z" and "S" shaped conformations exist in the opposite sides with respect to the ferrocenyl moiety. On the other hand, the two substituents in the "U" shaped one exist in the same side of the ferrocenyl moiety. It could be considered that the "Z" shaped conformation is the modified "S" shaped conformation.

In this study, monosubstituted ferrocene derivatives containing the same substituent of bMAF-*n* ($n = 2\sim12$) are prepared in order to compare the liquid crystallinity between the disubstituted ferrocene derivatives and the monosubstituted ones. A general structure of the monosubstituted ferrocene derivatives is shown in Figure 2. The name of the compound studied here is ω-[4-(4-methoxyphenoxycarbonyl)phenoxy]alkoxycarbonyl ferrocene (abbreviated hereafter as mMAF-*n*, where *n* means the same as that of bMAF-*n*).

In addition, a crystal structure analysis of mMAF-2 is carried out using single crystal X-ray diffraction method, because the structure analysis enables us to know interrelations between the crystal structure and some physical properties.

Experimental

A synthetic route of mMAF-*n* is shown in Figure 3. After purification using an open column chromatography, the products were identified as the objective compounds by ^{1}H-NMR (JEOL, ALPHA-400 (400 MHz)) spectrometer.

NMR data are as follows;

mMAF-2

^{1}H-NMR ($CDCl_3$) δ: 8.16 (d, 2H, $J = 8.8$ Hz), 7.11 (td, 2H, $J = 6.2, 4.1$ Hz), 7.05 (d, 2H, $J = 8.8$ Hz), 6.95–6.92 (m, 2H), 4.84 (t, 2H, $J = 1.7$ Hz), 4.62 (t, 2H,

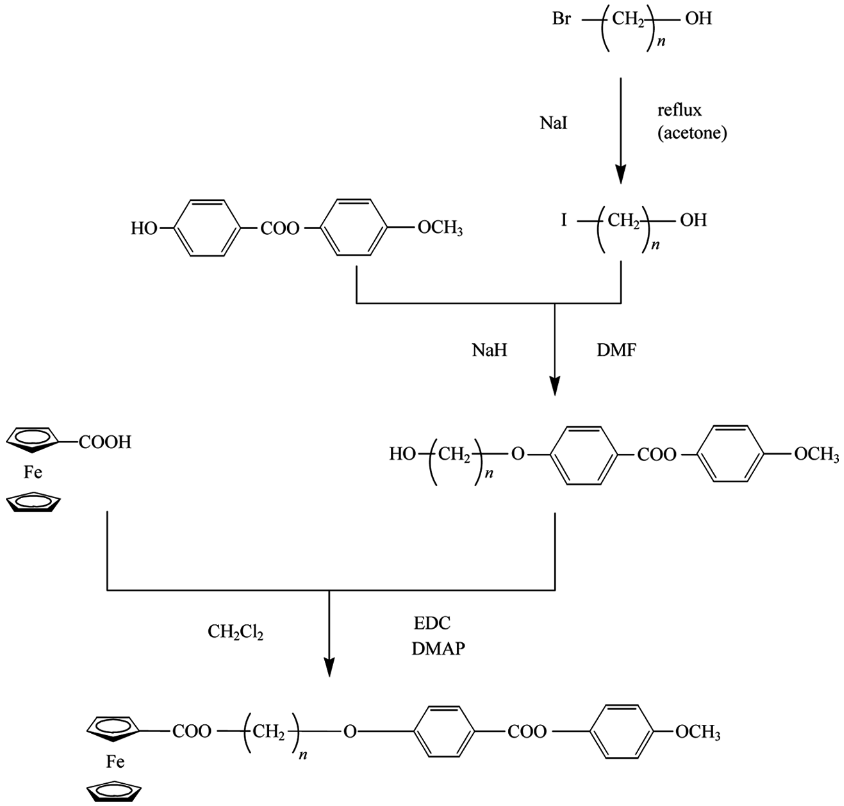

Figure 3. Synthetic route of mMAF-*n*, where *n* is the number of carbon atoms in the methylene chain.

$J=4.6$ Hz), 4.42 (t, 2H, $J=2.0$ Hz), 4.37 (t, 2H, $J=4.6$ Hz), 4.19 (s, 5H), 3.82 (s, 3H).

mMAF-3

^{1}H-NMR ($CDCl_3$) δ: 8.15 (d, 2H, $J=8.8$ Hz), 7.11 (dd, 2H, $J=6.8$, 2.0 Hz), 7.01 (d, 2H, $J=8.8$ Hz), 6.95–6.92 (m, 2H), 4.81 (t, 2H, $J=2.0$ Hz), 4.43 (dt, 4H, $J=13.2$, 4.1 Hz), 4.22 (t, 2H, $J=6.1$ Hz), 4.18 (d, 5H, $J=4.4$ Hz), 3.82 (s, 3H), 2.30–2.24 (m, 2H).

mMAF-4

^{1}H-NMR ($CDCl_3$) δ: 8.14 (d, 2H, $J=8.8$ Hz), 7.12 (t, 2H, $J=4.4$ Hz), 6.99 (d, 2H, $J=8.8$ Hz), 6.93 (d, 2H, $J=8.8$ Hz), 4.81 (t, 2H, $J=2.0$ Hz), 4.41 (t, 2H, $J=2.0$ Hz), 4.32 (t, 2H, $J=6.1$ Hz), 4.21 (s, 4H), 4.14 (t, 2H, $J=5.9$ Hz), 3.83 (s, 3H), 2.02–1.95 (m, 4H).

mMAF-5

^{1}H-NMR ($CDCl_3$) δ: 8.14–8.12 (m, 2H), 7.13–7.09 (m, 2H), 7.00–6.92 (m, 4H), 4.81 (t, 2H, $J=1.8$ Hz), 4.40 (t, 2H, $J=1.8$ Hz), 4.27 (t, 2H, $J=6.5$ Hz), 4.21 (s, 5H), 4.09 (t, 2H, $J=6.3$ Hz), 3.82 (s, 3H), 1.92 (q, 2H, $J=7.2$ Hz), 1.82 (dd, 2H, $J=14.6$, 6.6 Hz), 1.66 (q, 2H, $J=5.4$ Hz).

mMAF-6

^{1}H-NMR (CDCl$_3$) δ: 8.13 (d, 2H, $J = 8.8$ Hz), 7.12 (d, 2H, $J = 9.3$ Hz), 6.95 (dd, 4H, $J = 13.2$, 8.8 Hz), 4.81 (t, 2H, $J = 2.0$ Hz), 4.39 (t, 2H, $J = 1.7$ Hz), 4.24–4.22 (m, 7H), 4.10 (dd, 2H, $J = 18.5$, 12.2 Hz), 3.83 (s, 3H), 1.87 (d, 2H, $J = 8.8$ Hz), 1.79 (t, 2H, $J = 7.3$ Hz), 1.55 (s, 4H).

mMAF-7

^{1}H-NMR (CDCl$_3$) δ: 8.13 (d, 2H, $J = 8.3$ Hz), 7.12 (d, 2H, $J = 8.8$ Hz), 6.95 (dd, 4H, $J = 11.2$, 8.8 Hz), 4.81 (d, 2H, $J = 1.5$ Hz), 4.40 (d, 2H, $J = 1.5$ Hz), 4.22 (q, 7H, $J = 5.7$ Hz), 4.06 (t, 2H, $J = 6.3$ Hz), 3.83 (s, 3H), 1.86 (t, 2H, $J = 7.1$ Hz), 1.76 (t, 2H, $J = 7.1$ Hz), 1.51–1.48 (m, 6H).

mMAF-8

^{1}H-NMR (CDCl$_3$) δ: 8.13 (t, 2H, $J = 4.4$ Hz), 7.13–7.10 (m, 2H), 6.97–6.92 (m, 4H), 4.81 (t, 2H, $J = 2.0$ Hz), 4.39 (t, 2H, $J = 2.0$ Hz), 4.22 (q, 7H, $J = 5.2$ Hz), 4.04 (t, 2H, $J = 6.6$ Hz), 3.83 (s, 3H), 1.83 (q, 2H, $J = 7.0$ Hz), 1.74 (t, 2H, $J = 7.1$ Hz), 1.47 (d, 8H, $J = 21.0$ Hz).

mMAF-9

^{1}H-NMR (CDCl$_3$) δ: 8.13 (d, 2H, $J = 8.3$ Hz), 7.12 (d, 2H, $J = 8.3$ Hz), 6.95 (t, 4H, $J = 9.5$ Hz), 4.81 (d, 2H, $J = 1.5$ Hz), 4.39 (d, 2H, $J = 2.0$ Hz), 4.22 (q, 7H, $J = 4.4$ Hz), 4.04 (t, 2H, $J = 6.6$ Hz), 3.83 (s, 3H), 1.83 (t, 2H, $J = 7.6$ Hz), 1.74 (t, 2H, $J = 7.3$ Hz), 1.43 (d, 10H, $J = 33.2$ Hz).

mMAF-10

^{1}H-NMR (CDCl$_3$) δ: 8.13 (d, 2H, $J = 9.3$ Hz), 7.12 (t, 2H, $J = 4.4$ Hz), 6.95 (td, 4H, $J = 7.3$, 3.4 Hz), 4.81 (t, 2H, $J = 2.0$ Hz), 4.39 (t, 2H, $J = 2.0$ Hz), 4.22 (t, 7H, $J = 6.1$ Hz), 4.03 (t, 2H, $J = 6.6$ Hz), 3.82 (s, 3H), 1.85–1.79 (m, 2H), 1.72 (q, 2H, $J = 7.0$ Hz), 1.41 (d, 12H, $J = 44.9$ Hz).

mMAF-11

^{1}H-NMR (CDCl$_3$) δ: 8.13 (d, 2H, $J = 8.3$ Hz), 7.11 (d, 2H, $J = 8.8$ Hz), 6.95 (t, 4H, $J = 9.8$ Hz), 4.81 (d, 2H, $J = 2.0$ Hz), 4.39 (d, 2H, $J = 10.0$ Hz), 4.22–4.20 (m, 7H), 4.03 (t, 2H, $J = 6.6$ Hz), 3.82 (s, 3H), 1.82 (t, 2H, $J = 7.1$ Hz), 1.73 (t, 2H, $J = 7.1$ Hz), 1.45–1.34 (m, 12H).

mMAF-12

^{1}H-NMR (CDCl$_3$) δ: 8.13 (d, 2H, $J = 8.8$ Hz), 7.12 (d, 2H, $J = 8.8$ Hz), 6.95 (dd, 4H, $J = 11.2$, 8.8 Hz), 4.81 (s, 2H), 4.39 (s, 2H), 4.22–4.21 (m, 7H), 4.04 (t, 2H, $J = 6.3$ Hz), 3.83 (s, 3H), 1.82 (t, 1H, $J = 7.1$ Hz), 1.73 (t, 1H, $J = 7.3$ Hz), 1.45–1.31 (m, 13H).

Phase transition phenomena of mMAF-*n* were measured using Diamond DSC (Perkin Elmer) with heating and cooling rates of 5°C/min. The textures in the liquid crystalline phases were observed by a Nikon ECLIPSE E600 optical polarizing microscope equipped with a heating stage (Mettler Toledo FP90) of which heating and cooling rates are 5°C/min, as same as those of DSC measurements.

Single crystals of mMAF-2 were grown by the slow evaporation method from a mixed solvent solution of methylene chloride and ethanol (5:3). The single crystals obtained were block-like and orange in color. The sample, of which the dimensions were 0.50 × 0.32 × 0.17 mm, was mounted on a goniometer.

All measurements were carried out at the temperature, 296(2) K, using a Rigaku AFC-5*R* diffractometer with graphite-monochromated Cu $K\alpha$ radiation. The intensity data were corrected for Lorentz and polarization effects. Absorption corrections by Gaussian from the crystal shape [10] and decay corrections were applied. Secondary extinction corrections were also applied [11].

All non-hydrogen atoms were refined anisotropically. Isotropic displacement parameters of aromatic- and methylene-H atoms were set to be 1.2 U_{eq} of the parent atom, and those of methyl-H atoms were set to be 1.5 U_{eq}. The aromatic- and methylene-H atoms were located at idealized positions and were allowed to ride on the parent carbon atom (C–H = 0.93 Å for the aromatic parts, C–H = 0.97 Å for the methylene parts). The methyl-H atoms were located with idealized torsion angles by a rotating group refinement, and were allowed to ride on the parent carbon atom (C–H = 0.96 Å).

Computing Details

Data collection: *MSC/AFC Diffractometer Control Software* [12]; cell refinement: *MSC/AFC Diffractometer Control Software*; data reduction: *CrystalStructure* [13]; program(s) used to solve structure: *SIR*92 [14]; program(s) used to refine structure: *SHELXL*97 [11]; molecular graphics: *ORTEP*-3 *for Windows* [15]; software used to prepare material for publication: *WinGX* [16].

Results and Discussion

Phase Transition Behavior

Phase transition temperatures of mMAF-*n* ($n = 2 \sim 12$) obtained on cooling are shown in Figure 4. Only 4 members, that is mMAF-9~12, exhibited liquid crystalline phases, while the others were not shown. Every liquid crystalline member has two phases. The identification of liquid crystalline phases by polarizing microscopic observation is difficult, but it suggests that L.C.1 and L.C.2 are nematic phase and smectic one, respectively. These liquid crystalline phases are located around room temperature region and the temperature range is about 25–37°C.

Figure 5 shows a phase transition diagram of bMAF-*n* ($n = 2 \sim 12$) already reported [4]. Except bMAF-2 and 4, all the members showed a liquid crystalline phase. The bMAF-3 showed only nematic phase (L.C.1 in Figure 5) identified by polarizing microscopic observation in addition to X-ray measurement. The members of bMAF-5~10 exhibited two phases, L.C.1 and L.C.2, while the members of bMAF-11~12 had L.C.3 in addition to L.C.1 and L.C.2. From the polarizing microscopic observations and the X-ray measurements, L.C.2 and L.C.3 are regarded as smectic C and smectic F or I phases, respectively [4]. Here, pay attention that L.C.1 and L.C.2 in the Figures 4 and 5 are not the same.

From the results obtained by X-ray structure analyses of bMAF-*n*, it is considered that an aspect ratio of these liquid crystalline molecules is large enough to exhibit a liquid crystalline phase. The ratio is one of the most important factors to appear a liquid crystalline phase. Therefore, the members of bMAF-5~12 have the stable liquid crystalline phase of which temperature range is wider than that of the liquid crystalline mMAF-*n*. The liquid crystalline phase of the bMAF-*n* is located in rather higher region compared with that of the mMAF-*n*. In the case of

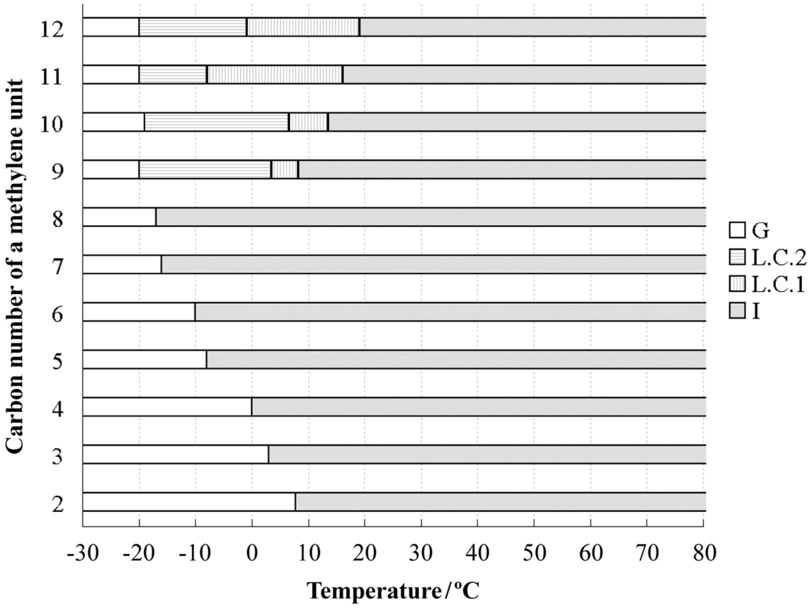

Figure 4. Phase transition behavior of mMAF-*n* (on cooling). I: Isotropic liquid; L.C.1: Liquid crystalline phase (~Nematic); L.C.2: Liquid crystalline phase (~Smectic); G: Glass state.

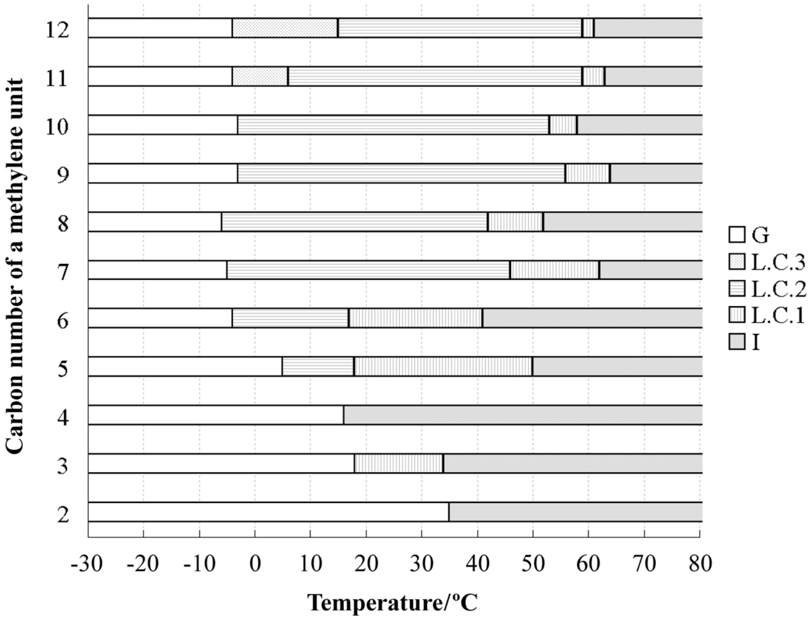

Figure 5. Phase transition behavior of bMAF-*n* (on cooling). I: Isotropic liquid; L.C.1: Liquid crystalline phase (Nematic); L.C.2: Liquid crystalline phase (Smectic C); L.C.3: Liquid crystalline phase (Smectic F or I); G: Glass state.

liquid crystalline bMAF-3 of which the length of substituent is not long enough, another reason may exist to show a liquid crystallinity.

In the series of bMAF-*n*, longer members tended to show a liquid crystalline phase, but shorter ones didn't, and the similar tendency was observed in the series of mMAF-*n*. Figure 6 showed a carbon number dependence of clearing temperatures of bMAF-*n* and mMAF-*n*. The clearing temperatures of bMAF-*n* increase with increasing the carbon number accompanying with a typical odd-even effect. The odd-even effect of bMAF-*n* became less remarkable with increasing the carbon number, and finally it converges to about 60°C [4]. In other word, no odd-even effect around bMAF-11∼12 was observed, though 11 is odd and 12 is even.

On the other hand, no odd-even effect was observed in the series of mMAF-*n*. The longer members, mMAF-9∼12, showed liquid crystalline phases. The mMAF-*n* has only two phenyl rings in the one mesogenic group, though the phenyl group of bMAF-*n* is a double because the number of mesogenic groups is two. As an existence of the phenyl ring is one of the most important factors to appear a liquid crystalline phase. Therefore, the mMAF-*n* is disadvantageous compared with the bMAF-*n*. Although a carbon number dependence of glass transition temperatures is not shown in Figure 6, it indicates a linear relation from 7.8°C of mMAF-2 through −17°C of mMAF-8. The glass transition temperatures of higher members, mMAF-9∼12, are about −18°C. If the curve of clearing points is extrapolated to lower members, it seems likely to appear a liquid crystalline phase around mMAF-7∼8. In fact, slightly small peaks were observed successively on a cooling DSC curve of mMAF-8 around 5°C. Although no texture change was detected in the polarizing microscopic observation around 5°C, these slightly small peaks may

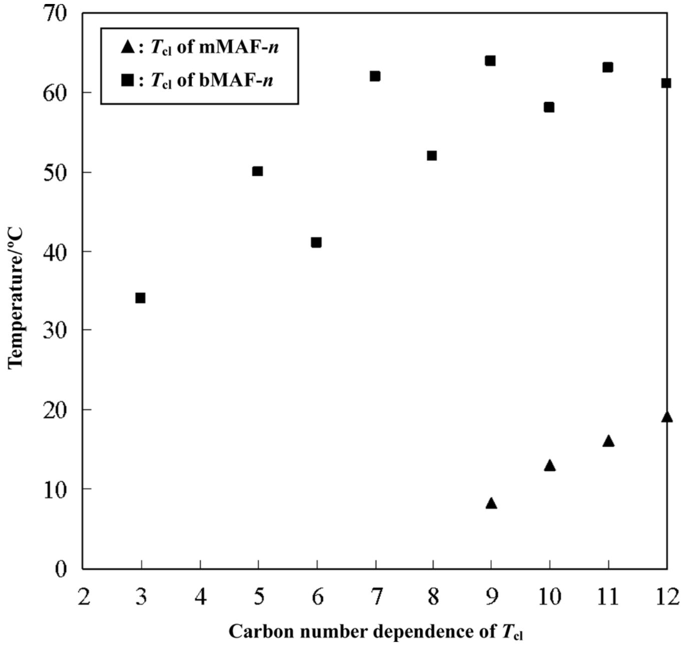

Figure 6. Carbon number dependence of clearing temperatures (T_{cl}) of bMAF-*n* and mMAF-*n* (on cooling).

Table 1. The summarized crystallographic data and the results of the final refinement of mMAF-2

Empirical formula	$C_{27}H_{24}FeO_6$
Formula weight	500.31
Crystal system	triclinic
Space group	P-1
a/Å	5.9118 (7)
b/Å	13.7485 (9)
c/Å	14.4799 (12)
α/°	86.019 (7)
β/°	87.113 (10)
γ/°	78.399 (7)
Volume/Å^3	1149.28 (18)
Z value	2
D_{calc}/gcm^{-3}	1.446
Measured reflections	4647
Independent reflections	4191
Parameters	309
Extinction coefficient	0.0069(4)
R	0.033
$wR(F^2)$	0.091
S	1.06

CCDC 707627 contains the supplementary crystallographic data for this paper. These data can be obtained free of charge *via* www.ccdc.cam.ac.uk/data_request/cif, or by emailing data_request@ccdc.cam.ac.uk, or by contacting The Cambridge Crystallographic Data Centre, 12, Union Road, Cambridge CB2 1EZ, UK; fax: +44 1223 336033.

correspond to the clearing and glass transition points. As a result, it needs to continue a careful survey on the liquid crystalline phase transition in mMAF-7∼8.

In order to discuss about the phase transition phenomena including the liquid crystalline phase transition in detail, the structure analysis of mMAF-2 was carried out as an example. The summarized crystallographic data and the results of the final refinement are shown in Table 1.

Molecular Structure

ORTEP-3 [15] drawing, the molecular structure of mMAF-2 with numbering for each atom is presented in Figure 6 where the hydrogen atoms are omitted for a simplification, together with that of bMAF-2 [5, (reproduced with the permission of Chemistry Letters, Copyright 2005, The Chemical Society of Japan.)] as a reference.

In the ferrocenyl moiety of mMAF-2, two cyclopentadienyl rings were almost parallel but not complete because the dihedral angle was calculated at 2.59(16)°. Two cyclopentadienyl rings assumed almost eclipsed conformation rather than staggered one. The eclipsed one has been found in monosubstituted ferrocene derivatives [17–21] of which the substituent structures are different from those of mMAF-*n*.

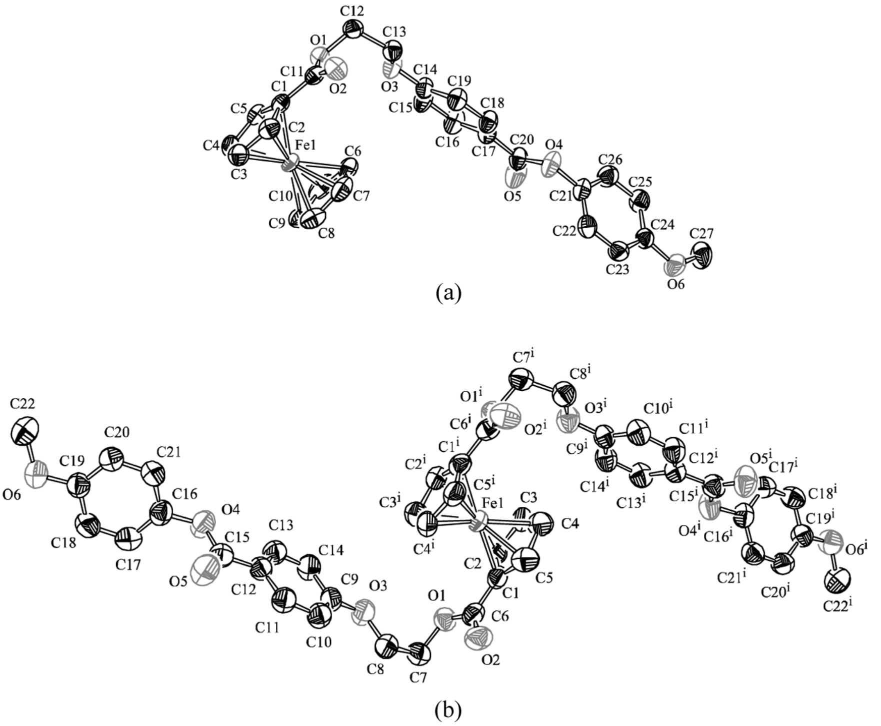

Figure 7. *ORTEP*-3 [15] views of the molecular structures excluding hydrogen atoms in (a) mMAF-2 and (b) bMAF-2 [5, (reproduced with the permission of Chemistry Letters, Copyright 2005, The Chemical Society of Japan.)]. Thermal ellipsoids are drawn at 50% probability.

The average values of the Fe-C and C-C bond distances in the ferrocenyl moiety of mMAF-2 were 2.036(7)Å and 1.408(13)Å, respectively. The C-C-C bond angles in the cyclopentadienyl rings were 108.0(8)° on average. These values are good agreement with those of ferrocene reported by Dunitz *et al.* [22] within an experimental error.

In the molecular structure of mMAF-2, the torsion angles of C(11)-O(1)-C(12)-C(13) and O(1)-C(12)-C(13)-O(3) showed the *gauche* conformation. As a result, the molecule bent over around the *gauche* conformation. This kind of bent structure is disadvantageous to showing a liquid crystalline phase. In fact, mMAF-2 didn't show a liquid crystalline phase as well as bMAF-2 [5]. As a topic of a great interest, the molecular structure of mMAF-2 is almost a half of that of bMAF-2, as is easily seen in Figure 7.

Crystal structure analyses of mMAF-*n* except mMAF-2 are now in progress. The results obtained will be discussed from a viewpoint of the phase transition behavior including that of mMAF-2.

References

[1] Carano, M., Chuard, T., Deschenaux, R., Even, M., Maraccio, M., Paolucci, F., Parato, M., & Roffia, S. (2002). *J. Matter. Chem.*, *12*, 829.

[2] Even, M., Heinrich, B., Guillon, D., Guldi, D. M., Parato, M., & Deschenaux, R. (2001). *Chem. Eur. J.*, *7*, 2595.

[3] Hanasaki, T., Ueda, M., & Nakamura, N. (1994). *Mol. Cryst. Liq. Cryst.*, *250*, 257.

[4] Nakamura, N., Mizoguchi, R., Ueda, M., & Hanasaki, T. (1998). *Mol. Cryst. Liq. Cryst.*, *312*, 127.

[5] Nakamura, N. & Nishikawa, M. (2005). *Chem. Lett.*, *34*, 1544.

[6] Okabe, T., Nakazaki, K., Igaue, T., Nakamura, N., Donnio, B., Guillon, D., & Gallani, J.-L. (2008). *J. Appl. Cryst.*, to be submitted.

[7] Nakamura, N., Okabe, T., & Takahashi, T. (2005). *Mol. Cryst. Liq. Cryst.*, *441*, 243.

[8] Nakamura, N., Nio, T., Okabe, T., Donnio, B., Guillon, D., & Gallani, J.-L. (2007). *Mol. Cryst. Liq. Cryst.*, *466*, 3.

[9] Nakamura, N. & Okabe, T. (2004). *Chem. Lett.*, *33*, 358.

[10] Coppens, P., Leiserowitz, L., & Rabinovich, D. (1965). *Acta Cryst.*, *18*, 1035–1038.

[11] Sheldrick, G. M. (2008). *Acta Cryst.*, *A64*, 112.

[12] Molecular Structure Corporation (1992). *MSC/AFC Diffractometer Control Software*. MSC, The Woodlands, Texas, USA.

[13] Molecular Structure Corporation & Rigaku. (2001). *CrystalStructure. Version 3.8.1*. MSC, The Woodlands, Texas, USA & Rigaku Corporation, Tokyo, Japan.

[14] Altomare, A., Cascarano, G., Giacovazzo, C., Guagliardi, A., Burla, M. C., Polidori, G., & Camalli, M. (1994). *J. Appl. Cryst.*, *27*, 435.

[15] Farrugia, L. J. (1997). *J. Appl. Cryst.*, *30*, 565.

[16] Farrugia, L. J. (1999). *J. Appl. Cryst.*, *32*, 837–838.

[17] Nakamura, N. & Setodoi, S. (1999). *Mol. Cryst. Liq. Cryst.*, *326*, 177.

[18] Nakamura, N. & Setodoi, S. (1998). *Mol. Cryst. Liq. Cryst.*, *319*, 173.

[19] Nakamura, N., Takahashi, T., Uno, K., & Hanasaki, T. (2002). *Mol. Cryst. Liq. Cryst.*, *383*, 27.

[20] Nakamura, N. & Setodoi, S. (1999). *Mol. Cryst. Liq. Cryst.*, *333*, 151.

[21] Nakamura, N., Setodoi, S., & Takayama, T. (2000). *Mol. Cryst. Liq. Cryst.*, *346*, 19.

[22] Dunitz, J. D., Orgel, L. E., & Rich, A. (1956). *Acta. Cryst.*, *9*, 373.